Earth and Planetary Science Letters 325–326 (2012) 108–115

Contents lists available at SciVerse ScienceDirect

Earth and Planetary Science Letters

journal homepage: www.elsevier.com/locate/epsl

An ikaite record of late Holocene climate at the Antarctic Peninsula

Zunli Lu [a,*], Rosalind E.M. Rickaby [b], Hilary Kennedy [c], Paul Kennedy [c], Richard D. Pancost [d], Samuel Shaw [e], Alistair Lennie [f], Julia Wellner [g], John B. Anderson [h]

[a] Department of Earth Sciences, Syracuse University, Syracuse, NY, 13244, USA
[b] Department of Earth Sciences, University of Oxford, South Parks Road, Oxford, OX1 3AN, UK
[c] School of Ocean Sciences, Bangor University, Menai Bridge, Anglesey, LL59 5AB, UK
[d] The Organic Geochemistry Unit, Bristol Biogeochemistry Research Centre, School of Chemistry, University of Bristol, Bristol BS8 1TS, UK
[e] School of Earth and Environment, University of Leeds, LS2 9JTddd, UK
[f] Diamond Light Source, Didcot, Oxfordshire, OX11 0DE, UK
[g] Department of Earth & Atmospheric Sciences, University of Houston, Houston, TX, USA
[h] Department of Earth Science, Rice University, Houston, TX, USA

ARTICLE INFO

Article history:
Received 9 August 2011
Received in revised form 18 January 2012
Accepted 31 January 2012
Available online 25 February 2012

Editor: G. Henderson

Keywords:
ikaite
hydration water
stable isotope
Holocene
Antarctic Peninsula

ABSTRACT

Calcium carbonate can crystallize in a hydrated form as ikaite at low temperatures. The hydration water in ikaite grown in laboratory experiments records the $\delta^{18}O$ of ambient water, a feature potentially useful for reconstructing $\delta^{18}O$ of local seawater. We report the first downcore $\delta^{18}O$ record of natural ikaite hydration waters and crystals collected from the Antarctic Peninsula (AP), a region sensitive to climate fluctuations. We are able to establish the zone of ikaite formation within shallow sediments, based on porewater chemical and isotopic data. Having constrained the depth of ikaite formation and $\delta^{18}O$ of ikaite crystals and hydration waters, we are able to infer local changes in fjord $\delta^{18}O$ versus time during the late Holocene. This ikaite record qualitatively supports that both the Medieval Warm Period and Little Ice Age extended to the Antarctic Peninsula.

1. Introduction

Ikaite is a low temperature polymorph of calcium carbonate that is hydrated with water molecules contained in its crystal lattice ($CaCO_3 \cdot 6H_2O$). Ikaite is thought to rapidly decompose into calcite and water at temperatures above 4 °C (Bischoff et al., 1993). Due to its stability only at near-freezing temperatures, ancient ikaite is commonly found decomposed into calcite pseudomorphs (glendonite), and is considered to be an indicator of cold glaciomarine environments (Selleck et al., 2007). More recent ikaite crystals are observed mainly in two settings. First, spectacular ikaite tufa towers in the shallow water column (<10 m) have been reported in the Ikka Fjord, Greenland (Buchardt et al., 1997; Hansen et al., 2011) and Mono Lake, California (Council and Bennett, 1993). Second, euhedral single crystals or stellate clusters (up to ~15 cm), have been found in marine sediments of the Zaire Fan (Jansen et al., 1987; Zabel and Schulz, 2001), Nankai Trough (Stein and Smith, 1986), Sea of Okhotsk (Greinert and Derkachev, 2004) and Bransfield Strait, Antarctic (Suess et al., 1982). These recent ikaite crystals from marine sediments, if collected and maintained at low temperatures, preserve hydration waters and their intact crystal structures, both of which have the potential to provide isotopic constraints on past climate change. Specifically the isotopic composition of the hydration waters may be used to reconstruct $\delta^{18}O$ of past porewaters, closely related to bottom water $\delta^{18}O$, which can yield insight into either the local or global history of ice sheets, depending on the sedimentary setting.

Laboratory synthesis experiments suggest that the hydration water in ikaite crystals faithfully records the oxygen isotope composition of the ambient water where the crystals form (Rickaby et al., 2006). If authigenic ikaite forms at depths close to the sediment water interface, the $\delta^{18}O$ composition of the hydration water may record snapshots of recent porewater $\delta^{18}O$ closely related to bottom water $\delta^{18}O$. Polar ice-sheet growth during the Last Glacial Maximum left a signature of isotopically enriched $\delta^{18}O$ in porewater profiles from the global deep oceans (Adkins et al., 2002; Schrag and Depaolo, 1993). Similarly, the most recent melting of the Caley Glacier on the AP during the last few decades released meltwater into nearby fjords and left a strong signal of negative $\delta^{18}O$ values in shallow porewater profiles (Lu et al., 2010). If ikaite crystals incorporate ambient porewaters into crystal structure as the hydration water, then crystals grown at different times will record the changes in bottom water $\delta^{18}O$ due to waxing and waning of (global or local) ice-

* Corresponding author.
E-mail address: zunlilu@syr.edu (Z. Lu).

0012-821X Published by Elsevier B.V. Open access under CC BY license.
doi:10.1016/j.epsl.2012.01.036

sheets. However, the finer details of how the meltwater entered the fjord and reached the bottom are beyond the scope of this study and cannot be resolved with our chemical data.

Here we present a hydration water and crystal $\delta^{18}O$ record from natural ikaite crystals collected from recent Antarctic Peninsula sediments, which makes a step toward establishing ikaite as a novel proxy for bottom water $\delta^{18}O$. U.S. Antarctic Program cruise NBP0703 collected piston cores around the AP and found ikaite crystals in multiple horizons at the Firth of Tay, Site JPC2, suitable for reconstructing a low resolution ikaite record of the last 2000 years (Fig. 1). Central questions we tackle in this paper include: (1) where does ikaite form in the sediment column; (2) does the hydration water of ikaite indicate bottom water conditions; (3) and does hydration water $\delta^{18}O$ provide climatic insight which is consistent with other climatic proxies?

We first show the depth profiles of $\delta^{18}O$ values for ikaite hydration waters ($\delta^{18}O_{hydra}$) and decomposed crystals (calcite, $\delta^{18}O_{CaCO3}$), to demonstrate that $\delta^{18}O_{hydra}$ preserves a signal of variability in the past. We use the porewater solute compositions (Ca, DIC) and coupled carbon isotope data ($\delta^{13}C_{DIC}$, $\delta^{13}C_{ikaite}$) to identify the formation depths of the ikaite crystals in the sediment column at JPC2 and then constrain the age difference between the ikaite crystals and the surrounding sediments. We then interpret the variability of the ikaite isotopic signals in terms of climatic change and show the consistency with other climatic indicators from the same core and from the Antarctic region.

2. Study area

Fig. 1 shows the studied area and location of sediment cores collected during the U.S. Antarctic Program cruise NBP0703. Of all sampled cores, two sites in the Bransfield Strait (JPC24) and the Firth of Tay (JPC2) were found to contain ikaite crystals. Ikaite was recovered from the Bransfield basin during a pioneer study by Suess et al. (1982). Because only one ikaite horizon was found in JPC24, we focus on reconstructing a record from Site JPC2 in Firth of Tay hereafter. The Firth of Tay is a narrow bay between Joinville Island and Dundee Island, at the northern tip of the AP (Fig. 1). Air temperature variations across this area suggest that ice close to the Firth of Tay might be sensitive to short-term climate changes (Vaughan and Doake, 1996). Up to 80 m of Holocene sediments fill the bay and accumulate on a few meters of till and proximal glaciomarine sediments, which rest directly on bedrock. The upper ~60 m of the Holocene section consists of organic-rich diatomaceous mud. *Chaetoceros* is the most abundant diatom genus found in the Firth of Tay (Michalchuk et al., 2009) and this genus is common in the AP region during the spring season when sea ice breaks up and nutrient availability is high at the sea ice edge (Leventer et al., 1996, 2002). The sedimentation rate in the ikaite bearing section (top 20 m) was determined to be 1 cm/yr (Michalchuk et al., 2009) from radiocarbon dating of the sparse carbonate fossil materials. Even with such a high deposition rate, it is challenging to resolve details of small-scale climate change as diagnostic indicators are largely absent in the sedimentary record. Carbonate fossil abundance is very low (<0.05wt.%) in most parts of the upper 20 m in JPC2 and ikaite crystals are the dominant sedimentary inorganic carbonate phase at this site. Ikaite occurrences have been previously reported at a nearby location southwest of the Firth of Tay, where four cores containing multiple ikaite crystals were collected. No large stable ikaite crystals were reported in any other cores collected in the Ross Sea or within the sediments of the East Antarctic shelf (Domack et al., 2007).

3. Samples and methods

3.1. Porewaters and sediments

A total of 41 porewater samples were collected from JPC2. They were extracted from ~1 m long core sections by cold centrifugation and filtered through a 0.2 μm filter immediately after core recovery. One portion of the porewater was stored in plastic centrifuge tubes and transported in airtight containers for nutrient and major ion analysis. The remaining porewater was stored in flame sealed glass ampoules, which had previously been poisoned with mercuric chloride, for analysis of dissolved inorganic carbon (DIC) and its carbon isotopic composition ($\delta^{13}C_{DIC}$). Porewater Ca concentrations were measured by ICP-MS (PerkinElmer Elan 6100), with a typical error of ~1%. The DIC concentrations and $\delta^{13}C_{DIC}$ were determined using an in-line manometer and a EUROPA PDZ 20/20 mass spectrometer, respectively. The stable carbon isotopic composition of sedimentary organic matter ($\delta^{13}C_{OM}$) was determined using homogenized and acidified sediments, via CO_2 gas produced from combustion in sealed tubes and separated from other gases, under vacuum, by cryodistillation. The precision of analyses on Dickson certified reference material batch #87 was 2000 ± 2 μM for DIC, $\delta^{13}C_{DIC}$ 0.7 ± 0.2‰ and $\delta^{13}C_{OM}$ ± 0.4‰ respectively.

3.2. Ikaite crystals

Site JPC2, at a water depth of 648 m in the Firth of Tay, proved to be an exceptional site for the formation of ikaite, and 11 crystals (2 to 6 cm in length, Fig. 2) were collected between 3.75 and 20 m below the sediment-water interface. The ikaite crystals were

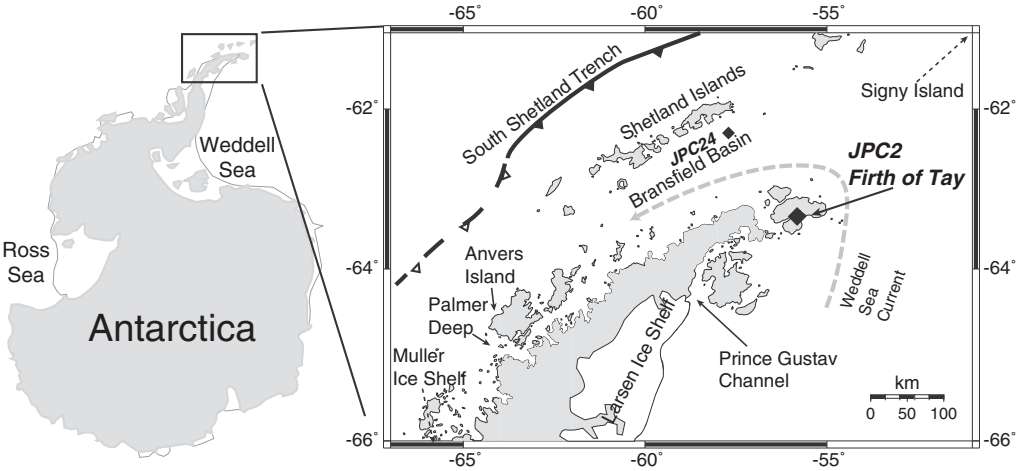

Fig. 1. Map of the Antarctic Peninsula. Large diamond shows location of JPC2. Locations for other climate records discussed in Fig. 4 are also indicated.

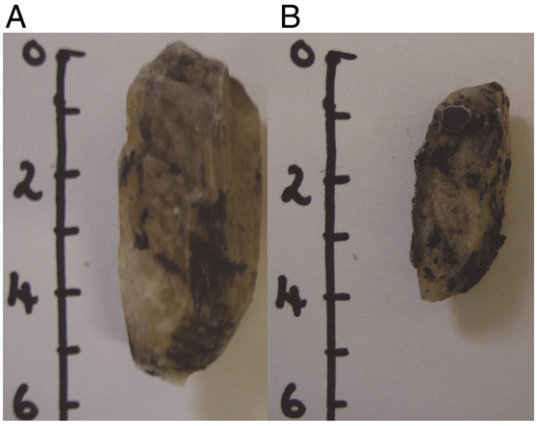

Fig. 2. Photos of ikaite crystals recovered at 6.5 m (A) and 9.4 m (B). Hand-drawn scales are in cm.

removed from the sediment and placed in 50 ml centrifuge tubes and stored at −28 °C without additional washing. In order to determine the chemical and isotopic composition of ikaite, crystals were weighed and crushed at 4 °C. The crushed crystals were placed in sealed centrifuge tubes for 30 min to decompose and extract hydration waters. The bottoms of the tubes were soaked in a water bath at 40 °C and the tops were cooled by ice. Nine $\delta^{18}O$ water standards of 0.2–1 ml were sealed and heated by the same method as applied on the crystals, serving as "process blanks" to monitor potential evaporation of hydration water during heating. The majority of heated process blanks yielded $\delta^{18}O$ values less than 0.1‰ heavier than those of unheated blanks, suggesting negligible alteration of $\delta^{18}O$ signal in our extraction method compared to the variability among our samples. Ikaite crystals were sub-sampled to provide between 0.5 and 1 g of water before decomposition. The yield of hydration waters was between 0.2 and 0.5 ml, close to complete extraction of waters based on the weight of residual carbonate. The oxygen isotope composition of the hydration waters ($\delta^{18}O_{hydra}$) and porewater ($\delta^{18}O_{pw}$) was analyzed on a Thermo Finnigan Delta V Advantage isotope ratio mass spectrometer (IRMS) using a Gas Bench II peripheral unit equipped with a PAL autosampler. Standards and samples were flushed for 6 min with 0.3% CO_2 in He, then left to equilibrate at 25 °C for 42 h before being analyzed. For water samples with a volume as small as 0.2 ml, a longer equilibration time of 42 h was required (Fig. 3). The analyses were calibrated against water standards from Iso-Analytical. Six repeated measurements on each sample (equilibrated gas) typically reach a precision better than ±0.1‰. The carbon and oxygen isotopic compositions of the

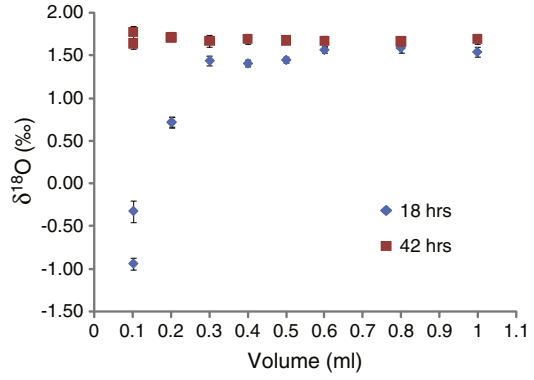

Fig. 3. Repeating $\delta^{18}O$ measurements on 18 splits of the same water sample with different volumes, after equilibration times of 18 h and 42 h respectively. Reliable $\delta^{18}O$ values can be obtained on water samples as small as 0.1 ml after 42 h of CO_2 equilibration.

decomposed ikaite crystals ($\delta^{18}O_{CaCO3}$ and $\delta^{13}C_{ikaite}$) were analyzed using a VG Isogas Prism II mass spectrometer with an on-line VG Isocarb common acid bath preparation system. Sub-samples were taken from different parts of the crystals and measured separately to examine the variability of $\delta^{13}C_{ikaite}$ in individual crystal.

4. Results and discussion

4.1. $\delta^{18}O_{hydra}$ preserves a signal of past porewater variability

New data produced in this study can be found in Tables 1 and 2. The downcore record of hydration water $\delta^{18}O_{hydra}$ and $\delta^{18}O_{CaCO3}$ shows some degree of covariance in timing, suggesting that the isotopic signatures of ikaite have captured and preserved some paleoenvironmental information at the time of their formation. The linear correlation coefficient (R^2) between $\delta^{18}O_{hydra}$ and $\delta^{18}O_{CaCO3}$ is 0.20, and the R^2 becomes 0.54 if the crystal at 11 m is excluded from the correlation. The downcore variations in $\delta^{18}O_{hydra}$ values (ranging from 0.84‰ to 4.17‰ SMOW) are much larger than the variability of $\delta^{18}O_{CaCO3}$ (32.81–34.00‰ SMOW). $\delta^{18}O_{hydra}$ values increased by about 5‰ at 10–15 m, which will be discussed later.

The $\delta^{18}O_{hydra}$ show no signs of significant exchange with porewater $\delta^{18}O$. If we assume that post-crystallization isotopic alteration occurs via exchange only and does not incur the same fractionation as during initial crystallization, then $\delta^{18}O_{hydra}$ would decrease with

Table 1
Chemical and isotopic compositions of porewaters in site JPC2.

Section	Depth (cm)	Depth (cm)	SO_4 (mM)	Ca (mM)	DIC (mM)	$\delta^{13}C_{DIC}$ PDB (‰)
1A	0	1	27.3	9.00	4.8	−10.2
1A	50	50	25.9	9.30	8.8	−13.7
1A	100	100	24.9	9.61	10.7	−14.8
1A	150	150	19.8	9.33	15.9	−17.6
1B	0	160	18.1	9.04	17.5	−18.1
1B	50	205	4.9	4.43	32.6	−19.7
1B	100	255	0.7	2.10	40.9	−9.2
1B	150	305	0.7	2.30	45.1	−2.0
2A	10	315	1.4	2.88	43.3	−1.5
2A	30	335	1.9	3.79	44.1	−0.3
2A	50	355	1.1	3.25	45.9	1.3
2A	70	375	0.8	3.57		
2B	20	407	1.1	2.42		
2B	60	447	0.7	2.16		
2B	100	487	0.4	3.96		
2C	40	539	0.5	4.37		
2C	80	579	1.7	2.20		
3A	20	605	0.6	1.73		
3A	65	650	0.8	0.83		
3B	10	697	1.0	0.75	60.3	9.6
3B	60	747	0.8	1.16		
3C	30	820		1.08		
3C	80	870	1.0	1.01		
4A	10	902				
4A	50	942				
4B	10	998				
4B	60	1048	1.5	1.38		
4C	15	1107				
4C	65	1157	0.1	0.52		
5A	10	1204				
5A	60	1254		0.35		
5B	30	1325				
5B	90	1385				
5C	20	1414	0.1	1.44		
5C	70	1464	0.1	1.28		
6A	66	1565	0.1	1.01		
6B	60	1661	0.1	1.41		
6C	60	1762			76.1	13.3
7A	45	1848				
7B	30	1937	0.1	0.96		
7C	50	1994		0.58		

Table 2
Carbon and oxygen isotopic compositions of ikaite crystals in site JPC2.

Section	Depth (cm)	Depth (cm)	Weights (g)	$\delta^{18}O_{hydra}$ SMOW (‰)	$\delta^{18}O_{CaCO3}$ PDB (‰)	$\delta^{18}O_{CaCO3}$ SMOW (‰)	$\delta^{18}O_{ppw}$ SMOW ‰)	$\alpha_{Caco3\text{-}ppw}$ SMOW	$\delta^{13}C_{ikaite}$ PDB (‰)	Formation depth
2A	70	375	4.7	2.43	1.85	32.81	−0.47	1.0333	0.6	345
2B	20	407	4.7	2.13	2.19	33.16	−0.77	1.0340	−0.20, 1.01	341
3A	65	650	13.5	3.43	2.63	33.62	0.53	1.0331	−13.89	236
3C	30	820		1.63	1.92	32.89	−1.65	1.0346	3.60, 4.38	372
4A	50	942	4.0	1.54	2.11	33.09	−1.36	1.0345	−0.03	324
4C	15	1107		0.84	2.65	33.64	−2.06	1.0358	3.04, 3.88	364
5B	85	1385	6.9	3.50			0.60			304
5C	70	1464	5.8	4.10	3.00	34.00	1.20	1.0328	−16.97	217
6A	66	1565	1.0	3.96	2.63	33.62	1.06	1.0325	−1.63, −0.92	314
7A	45	1848	13.8	4.17	2.58	33.57	1.27	1.0323	−2.93	306
7C	45	1994	8.9	3.86	2.08	33.06	0.96	1.0321	0.19	275
									Average:	304 ± 57

depth and gradually approach lighter values of $\delta^{18}O_{pw}$. Such a trend is not observed in our data (Fig. 4A). Furthermore, experimental uncertainty and natural variability within the crystal should not introduce large artifacts into the depth trend, since separate analyses on three crystals found in the same horizon at the other Bransfield Strait site, Site JPC24, yield $\delta^{18}O_{hydra}$ values of 3.92 ± 0.33‰.

The fractionation factor (α) between hydration water $\delta^{18}O_{hydra}$ of the shallowest (most recent) crystal and modern porewater $\delta^{18}O_{pw}$ matches the fractionation factor ($\alpha = 1.0029 \pm 0.0002$) obtained in the laboratory ikaite synthesis experiments (Rickaby et al., 2006). Such consistency suggests that the hydration water in natural crystal also potentially records ambient porewater $\delta^{18}O$. Six crystals capture similar $\delta^{18}O_{hydra}$ values of ~4‰, four from the lower part of the core (>13 m, Fig. 4A) and one at 6.5 m. The other five crystals are characterized by $\delta^{18}O_{hydra}$ values that are significantly lighter with values of (~1‰) between 12 and 8 m, and the two shallowest crystals with $\delta^{18}O_{hydra}$ values of 2.1–2.4‰. The downcore trends in $\delta^{18}O_{CaCO3}$ and $\delta^{18}O_{hydra}$ are in general agreement, although the variability of $\delta^{18}O_{CaCO3}$ is significantly smaller (<1.2‰, Fig. 4A). From the shallowest crystal, we find a fractionation factor for oxygen isotopes into the carbonate of ikaite crystals ($\alpha_{CaCO3\text{-}ppw}$) of 1.0333 (SMOW), of comparable magnitude to that of calcite precipitation at 0 °C (1.0324) (Kim and ONeil, 1997). Paleo-porewater $\delta^{18}O_{ppw}$ can be calculated using $\delta^{18}O_{hydra}$ plus 2.9‰, which allows us to further calculate $\alpha_{CaCO3\text{-}ppw}$ for ikaite carbonate and paleo-porewater. Downcore $\alpha_{CaCO3\text{-}ppw}$ varies between 1.0332 and 1.0336 and appears to be closely correlated to $\delta^{18}O_{hydra}$ ($R^2 = 0.91$) with higher $\alpha_{CaCO3\text{-}ppw}$ corresponding to lighter $\delta^{18}O_{hydra}$ (Fig. 4B), suggesting that the two signatures are driven by a common factor. Before we interpret these records in terms of climate we must establish the age of the ikaite crystals with respect to the ambient sediment.

4.2. Ikaite formation depth

Ikaite formed close to the seafloor holds the best potential to capture subtle climate changes, expressed as change in the input of isotopically light meltwater to the fjord and ultimately change in bottom water $\delta^{18}O$. Previous studies have used porewater Ca, DIC concentrations and alkalinity to constrain the depth of ikaite precipitation in the sediment column (Suess et al., 1982; Zabel and Schulz, 2001). Organic matter diagenesis raises dissolved inorganic carbon (DIC) content in the porewater. If the porewaters become super-saturated with respect to carbonate minerals, precipitation occurs and the mineral's carbon isotope composition reflects the diagenetic setting at that depth. The wide range of previously measured $\delta^{13}C$ values for ikaite collected from marine sediments (+0.9 to −36.3‰) suggests that ikaite can precipitate from a range of diagenetic settings (Jansen et al., 1987; Schubert et al., 1997; Stein and Smith, 1986; Suess et al., 1982). We use a similar approach, based firstly on the geochemistry of the porewaters and secondly on the $\delta^{13}C$, to show

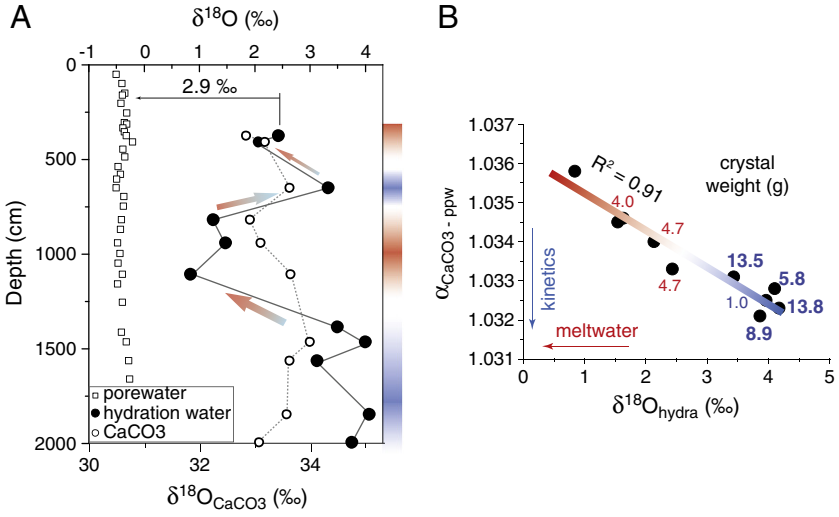

Fig. 4. A: $\delta^{18}O$ depth profile of hydration water, decomposed ikaite crystal (calcite) and modern porewater. All in VSMOW (but note the two scales for the x-axes for carbonate and water). Blue and red bars show the interval of cold and warm conditions indicated by $\delta^{18}O_{hydra}$. B: $\alpha_{CaCO3\text{-}ppw}$ plotted against $\delta^{18}O_{hydra}$, showing a trend likely due to kinetic effect on oxygen isotope fractionation (higher ikaite growth rate at lower temperature). Numbers are the crystal weights in grams.

that each ikaite crystal intermittently distributed throughout JPC2 was formed very rapidly at 2–4 m sediment depth. The age of the ikaite crystal is younger than the surrounding sediments by the length of time taken for sediment to be buried to 2–4 m.

Porewater Ca and DIC concentrations show reverse depth trends and the two profiles cross each other around the sulfate methane transition (SMT) (Fig. 5A–B), which is just above the shallowest ikaite horizon. Zabel and Schulz (2001) reported that the only ikaite crystal in the entire core at the Congo Fan was also found close to the SMT coinciding with the highest [Ca][DIC] value throughout the core. The most plausible explanation is that ikaite saturation ($\Omega = [Ca^{2+}][CO_3^{2-}]/K^*_{ikaite}$) depends on the DIC level increasing above ~40 mM (at local pH) and rapid carbonate precipitation removes dissolved Ca from the porewater around the SMT. At JPC2, further ikaite growth during burial is unlikely as Ca concentration remains low beneath 5 m. Because the ikaite saturation and crystal growth are limited by both Ca and DIC, the zone of "trade-off" between these two concentrations close to the SMT should be where most of the crystals formed, according to the porewater profiles. We cannot calculate downcore Ω values without pH data and precise correction formula is not available for K^*_{ikaite} at different temperature and salinity conditions. However no crystal dissolution was observed below the SMT, which probably is related to high phosphate concentrations (Supplementary file, Fig. S1) stabilizing ikaite crystals as shown in laboratory experiments (Bischoff et al., 1993).

The coupled carbon isotope compositions of porewaters and crystals support the interpreted depth of the ikaite formation zone and allow more precise determination of the formation depth for each crystal (Fig. 5C). We assumed that the fractionation between ikaite and the DIC is small, similar to calcite (Romanek et al., 1992), so that $\delta^{13}C_{ikaite}$ reflects the $\delta^{13}C_{DIC}$ of the porewater carbon pool from which the crystals precipitated. Kinetic controls probably also have a small influence due to the large range and steep slope of the porewater $\delta^{13}C_{DIC}$ profile. The porewater $\delta^{13}C_{DIC}$ exhibit large variations in JPC2 between −20‰ and +13.3‰ (Fig. 5C). The ikaite crystals analyzed from JPC2 fall in a range of −17.0‰ to +4.4‰. The majority of the crystals from JPC2 have relatively positive $\delta^{13}C$ values between −3‰ and +5‰, except for two crystals found at 6.5 m (−14.0‰) and 14.6 m (−17.0‰). The $\delta^{13}C_{DIC}$ profile was broken down to three segments and fitted with three numerical functions (Fig. 5C). The formation depth can then be calculated using $\delta^{13}C_{ikaite}$ of each crystal. Two crystals with light $\delta^{13}C_{DIC}$ can be fitted to both above and below SMT. We manually selected the formation depth at higher saturation (higher [Ca][DIC]). Thus, we are able to estimate the formation depth for each crystal. Most crystals with relatively positive $\delta^{13}C_{ikaite}$ values formed between 3 and 4 m. The ones with very light $\delta^{13}C_{ikaite}$ values likely precipitated at 2–2.5 m.

Uncertainties in the ikaite formation depth estimated by $\delta^{13}C_{ikaite}$ chemostratigraphy are mainly related two factors: ikaite growth rate and the stability of SMT depth. Accurate estimate of growth rates for JPC2 is not possible at present. However, where Ca is not limited, such as in the Ikka Fjord, ikaite towers can grow up to 50 cm/yr. Ikaite synthesis experiments in laboratory conditions also easily yield crystals >1 mm over 10–15 h (Supplementary file, Fig. S2). The crystals collected in JPC2 have dimensions between 3 cm×1 cm and 4.5 cm×1.5 cm. Each of these crystals might have grown within a few decades. Therefore, $\delta^{18}O$ of each ikaite can be regarded as a decadal snapshot of the shallow porewater conditions over time. If the crystals continued to grow significantly in size utilizing porewater DIC at depth much greater than the SMT, measured $\delta^{13}C_{ikaite}$ values would increase downcore, which is not supported by our data. Different parts of each crystal that were sub-sampled had very small variations (0.9‰) in $\delta^{13}C$ values (Fig. 5C), again suggesting that individual crystal growth cannot occur over a broad depth range due to the lack of Ca in deep porewater. The kinetic effect of carbon isotope fractionation during crystallization should only have a minor influence on the calculated formation depths, because of the sharp gradient in the $\delta^{13}C_{DIC}$ profile. For calcite, the kinetic influence on $\delta^{13}C$ fractionation was shown to be less than 3‰ (Turner, 1982). If we consider a kinetic fractionation of 5‰ for ikaite that would only change formation depths by roughly 30 cm for crystals with negative $\delta^{13}C_{ikaite}$ values.

The shape of $\delta^{13}C_{DIC}$ profile might have been different in the past, which would introduce error when we match $\delta^{13}C_{ikaite}$ with the modern $\delta^{13}C_{DIC}$ profile to constrain crystal formation depth. The main control of the negative excursion in $\delta^{13}C_{DIC}$ profile is the SMT, where ^{13}C depleted methane is converted into DIC. The SMT depth is influenced by the rate of organic matter degradation, the relative fluxes of sulfate and methane, sedimentation rate and flow rate (Hensen et al., 2003; Wallmann et al., 2006). However, rather invariant concentrations of pentamethylicosane (PMI, a biomarker for anaerobic methane oxidation) argue against large scale, past changes in DIC and $\delta^{13}C_{DIC}$ profiles (Supplementary file, Fig. S3) in JPC2, although we cannot rule out minor shifts in the SMT depth.

4.3. $\delta^{13}C$ chemostratigraphy for ikaite ages

To compare the ikaite $\delta^{18}O$ data with other climate records, the ikaite crystals need to be dated but there are obvious problems applying prevailing carbonate dating tools to obtain ikaite ages. The radiocarbon method does not reflect the time of crystal formation; it can

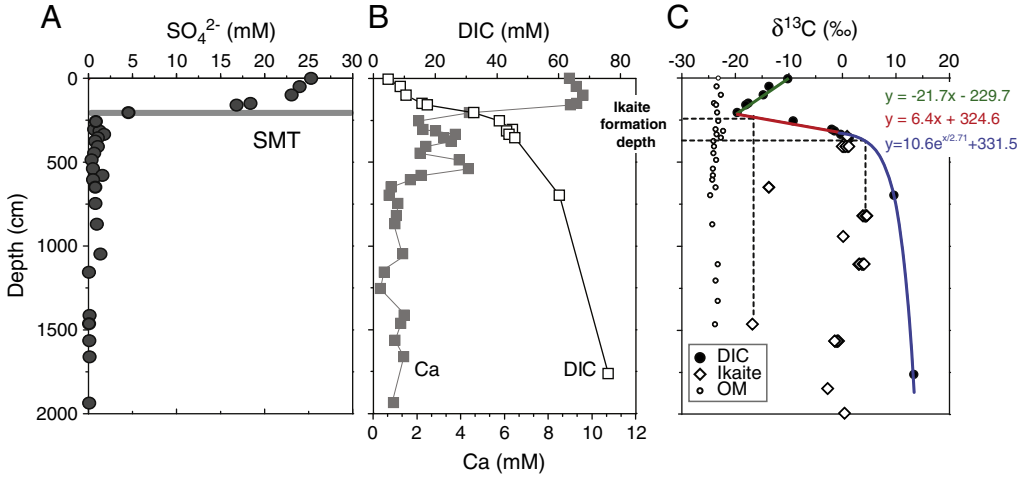

Fig. 5. A–B: Depth profiles of porewater SO_4^{2-}, Ca and DIC concentrations. SMT shows the depth of sulfate methane transition. C: $\delta^{13}C$ of DIC, ikaite crystals, sedimentary organic matters, and inferred ikaite formation zone. The $\delta^{13}C_{DIC}$ profile was fitted with three numerical functions for calculating crystal formation depths.

only estimate the age of DIC locked in ikaite. This kind of DIC age is essentially the averaged age for organic carbon and methane released from sediments much deeper than the ikaite formation zone. U–Th dating also cannot be applied due to relatively high levels of terrestrial material. However the sedimentation rate at Firth of Tay has been well constrained to be 1 cm/yr by radiocarbon dating of carbonate fossils (Michalchuk et al., 2009). We can estimate the time of crystallization using ikaite formation depth and the known sediment accumulation rates, because the age of ikaite will always be younger than its host sediment by the amount of time taken for the sediment to be buried to the depth of the ikaite formation zone. Considering the potential uncertainty in crystal formation depth fitted by $\delta^{13}C$ chemostratigraphy, we apply the averaged formation depth of 3.04 $\pm$0.57 m to calculate ages of all crystals. This approach offsets ikaite ages by ~300 yrs from the host sediments in which crystals are found. Based on these assumptions, the calculated ages for the ikaite crystals range between 74$\pm$60 and 1760$\pm$60 yrs. The kinetic effect of $\delta^{13}C$ and formation depth (30 cm) would not cause age uncertainties larger than the quoted error of $\pm$60 yrs.

4.4. Isotopic signatures of ikaite indicating climate changes?

Assuming that lighter $\delta^{18}O_{hydra}$ values reflect warmer climate on the AP, which induces increased drainage of meltwaters to the Firth of Tay, the ikaite record can be interpreted as a prolonged cold period dominating the older part of the core, followed by an oscillation to a period of warmth, a return to cold conditions and a final trend of increasing warmth (Fig. 4A). Given the correlation of $\delta^{18}O_{hydra}$ with $\alpha_{CaCO3\text{-}ppw}$, temperature should underlie the variance of both records. However, if the $\delta^{18}O_{CaCO3}$ conformed to equilibrium expectations, then $\alpha_{CaCO3\text{-}ppw}$ should decrease with increasing temperature, the exact inverse of what is found (Fig. 4B). If our interpretation of $\delta^{18}O_{hydra}$ variability with changing climate is correct, the most reasonable explanation for such an inverse relationship of $\alpha_{CaCO3\text{-}ppw}$ with temperature is that kinetics exert an important control on the $\delta^{18}O_{CaCO3}$. Two pieces of evidence support this proposal that the faster growing crystals yield lighter isotopes within the carbonate due to a smaller $\alpha_{CaCO3\text{-}ppw}$ (Dietzel et al., 2009). First, because ikaite is less soluble at lower temperature (Bischoff et al., 1993) and mineral growth rate is typically controlled by saturation state, the ikaite crystals should grow faster during the colder periods (easier to reach super-saturation). Second, if we can use downcore variations in the weights of crystals, as a qualitative indicator of the growth rate of those crystals, the larger crystals with heavier $\delta^{18}O_{CaCO3}$ also correspond to the periods of coldest temperature, heavier $\delta^{18}O_{hydra}$ values and smallest $\alpha_{CaCO3\text{-}ppw}$ (Fig. 4B).

Although there appears to be no systematic isotopic exchange between $\delta^{18}O_{hydra}$ and $\delta^{18}O_{pw}$ during crystal burial, we cannot rule out this effect for individual crystals, especially those with light $\delta^{18}O_{hydra}$ values. Because warmer temperatures destabilize the ikaite structure, exchange of $\delta^{18}O_{hydra}$ signature may be more likely during warm periods and probably could further amplify the light $\delta^{18}O_{hydra}$ signal caused by meltwater. Such a consideration does not change the interpretation that light values of $\delta^{18}O_{hydra}$ qualitatively indicate meltwater input as a result of regional warming.

The correlation between $\delta^{18}O_{hydra}$, $\delta^{18}O_{CaCO3}$, and ikaite weights, allows us to translate both isotopic signals to regional warming (cooling) versus time. Any meltwater signal of light $\delta^{18}O_{ppw}$ would generally be smoothed out by diffusion within 100 years depending on the scale of the melting event (Lu et al., 2010). Since the accumulation of sediments between neighboring crystals in JPC2 took generally more than 100 yrs, each crystal should record the condition during its formation without much residual influence of previous meltwater events. We consider our trends in ikaite $\delta^{18}O$ in the framework of Late Holocene paleoenvironmental changes which have been previously compiled by Bentley et al. (2009). After the Mid-Holocene warmth, cooling signals were found in different parts of the AP at various times between 2.5 and 1.2 ka, followed by the Medieval Warm Period (MWP, 1.2–0.6 ka) and the Little Ice Age (LIA) (Bentley et al., 2009). The cooling–warming trends indicated by $\delta^{18}O_{hydra}$ and $\alpha_{CaCO3\text{-}ppw}$ values appear to be in good agreement with this climate pattern. Here we compare the ikaite record to the magnetic susceptibility (MS) and TOC in JPC2 (Michalchuk et al., 2009), other climate records in the AP region, and the EPICA ice-core $\delta^{18}O$ values as a general climate index for the entire Antarctic area, in order to show how the level of consistency changes as we look at a single site versus a broader region. (Fig. 6A–E). We suggest that the ikaite record at Firth of Tay provides an additional piece of evidence to support the expression of the MWP in Southern Hemisphere and the northernmost AP also bears the imprint of the LIA.

Crystals older than 1.1 ka have unanimously high $\delta^{18}O_{hydra}$ values indicating a cool climate at Firth of Tay, which is supported by consistently higher MS and lower TOC compared to the average value in the last 2000 yrs (Fig. 6A–B). South of JPC2 on the east AP, glaciers

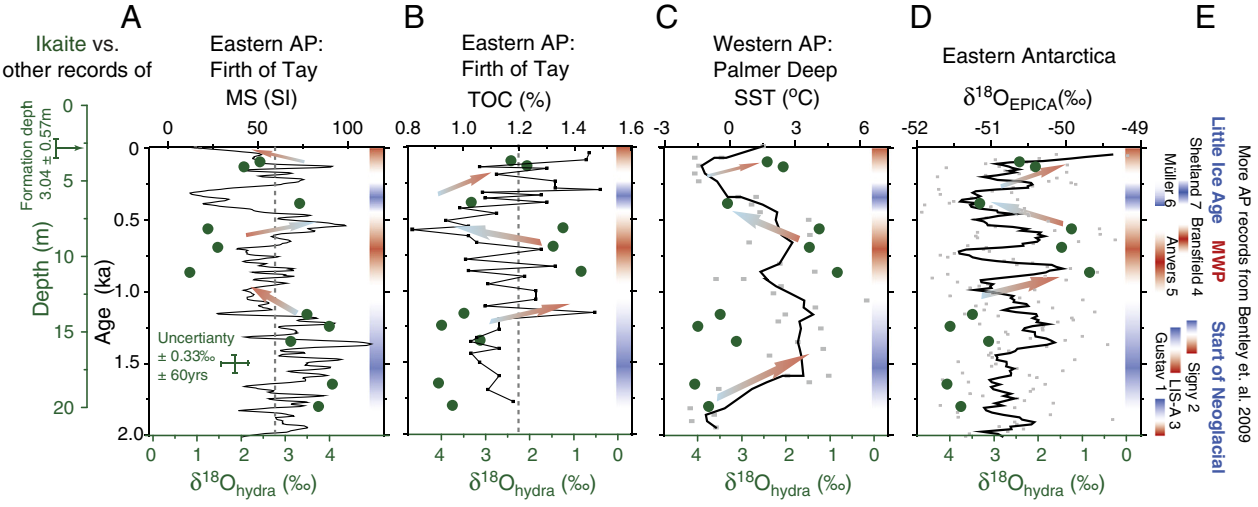

Fig. 6. $\delta^{18}O_{hydra}$ profile (in green) plotted with other climate records, assuming sedimentation rate of 0.96 cm/yr and ikaite formation depth of 3.04$\pm$0.57 m. $\delta^{18}O_{hydra}$ variability among different crystals found at the same depth is about $\pm$0.33‰. A–B: Magnetic susceptibility and TOC of JPC2 are plotted against age. C: SST at Palmer Deep, the line represents a five-point moving average (Shevenell et al., 2011). D: $\delta^{18}O_{EPICA}$ data are smoothed by a ten-point moving average. E: Timing of climatic events summarized for the AP region and citations (1 — Pudsey and Evans (2001); 2 — Jones et al. (2000); 3 — Brachfeld et al. (2003); 4 — Khim et al. (2002); 5 — Hall et al. (2010); 6 — Domack et al. (1995); 7 — Liu et al. (2005)). See Fig. 1 for locations of these studies.

flowing into Prince Gustav Channel and Larsen-A Ice Shelf started to reform at 1.9 ka (Pudsey and Evans, 2001) and 1.4 ± 0.25 ka (Brachfeld et al., 2003). Macrofossil abundance began to decline at 1.5–1.3 ka on Signy Island, further north in the Weddell Sea (Jones et al., 2000), also supporting the development of colder condition in the area. $\delta^{18}O_{EPICA}$ (Stenni et al., 2006), as an indicator of general Antarctic climate, showed a cold period from 2 ka to 1.5 ka (Fig. 6D). However, SST increased by over 3 °C at Palmer Deep, on the west side of AP (Fig. 6C), indicating complex climate variability across the AP (Shevenell et al., 2011).

The MWP has not yet been unambiguously established around the AP. Three $\delta^{18}O_{hydra}$ values fall in this period and all of them are significantly lighter than those values of older crystals by 2–3‰, a difference too large to be explained by analytical uncertainties and variability among crystals formed at the same time (0.33‰ at JPC24), and are associated with lower $\delta^{18}O_{CaCO3}$. We tentatively interpret this shift in ikaite isotopic values as the result of meltwater invasion, and warming in the Firth of Tay during the MWP. The ~5‰ decrease in $\delta^{18}O_{hydra}$ at the beginning of the MWP must indicate very strong freshening at the bottom of fjord, likely due to meltwater cascading to depth. How such a distinct isotopic signal might be preserved to such great depth in the fjord is beyond the scope of this paper. However, meltwater beneath the ice-sheet is known to be injected into fjords at different water depths including the base of the fjord (Domack and Ishman, 1993). Although meltwater typically mixes quickly with fjord water, it can be trapped at the base of the inner fjord sometimes (e.g. when there is a sill preventing it from moving forward) (Domack and Ishman, 1993). We hypothesize that such subglacial meltwater may be the cause of strong meltwater signal at the beginning of MWP. Other evidence supports the meltwater signal inferred from $\delta^{18}O_{hydra}$. At the Firth of Tay, MS shifted to mostly below average values between 1 and 0.6 ka (Fig. 6A). Low MS was also found for the same period of time in Bransfield Strait sediments and was considered to mark the MWP (Khim et al., 2002). Elemental ratio records from Maxwell Bay, northern Bransfield Strait, allow identification of both the MWP and the Little Ice Age (Monien et al., 2011). Moss exposed by recent ice retreat on Anvers Island, West AP, were radiocarbon dated to 0.7–0.97 ka, contrary to the much older ages of reworked marine shells in the same sections, indicating that the ice-sheet was reduced during that period to an extent of similar magnitude to today (Hall et al., 2010). $\delta^{18}O_{EPICA}$ (Stenni et al., 2006) shows warming at 0.6–0.8 ka, but with a brief cooling in between. SST at Palmer Deep was even higher than modern during this period (Shevenell et al., 2011). There is a notable lag between the onset of MWP at the western AP and at the eastern AP according to this SST record and our ikaite record although this observation needs to be confirmed by additional records. On the eastern AP, no significant change in foraminifera assemblage at Firth of Tay was observed that could correspond with the Medieval Warm Period, Little Ice Age, or the warming over the last century (Majewski and Anderson, 2009). Also signals of the MWP or LIA, if any, were not up to a magnitude that influenced glacial sedimentation (Michalchuk et al., 2009).

The LIA has been recognized in the AP region broadly between 700 and 150 yrs B.P. (Bentley et al., 2009; Domack et al., 1995; Liu et al., 2005), in sediment cores and glacial advances. Our only ikaite crystal formed during LIA does indicate significant cooling relative to the MWP. A relatively low TOC level in the LIA interval was consistent with ikaite data, although the lowest TOC values were found at a slightly older level (Fig. 6B). $\delta^{18}O_{EPICA}$ (Stenni et al., 2006) and SST at Palmer Deep (Shevenell et al., 2011) both indicate colder climate during LIA. Magnetic susceptibility in JPC2 showed a rapid increase at the initial LIA and a reversed shift during most part of this event, although MS records in the nearby Bransfield Basin (Khim et al., 2002), demonstrated a convincing signal of LIA. However other investigations found no compelling sedimentological evidence for LIA in Maxwell Bay, South Shetland Island (Heroy et al., 2008; Milliken et al., 2009). Our most recent crystals suggest a warming relative to the LIA in the last century, possibly as part of the regional recent rapid warming, but this climatic signature is not yet as extreme in nature as the MWP. The resolution of our record is insufficient to constrain the ages of these climatic oscillations in the Southern hemisphere relative to their expression in the Northern hemisphere, but our ikaite record builds the case that the oscillations of the MWP and LIA are global in their extent and their impact reaches as far South as the Antarctic Peninsula, while prior studies in the AP region have had mixed results.

5. Conclusions

We report the first comprehensive geochemical study on an ikaite-containing core to demonstrate the potential of using hydration water $\delta^{18}O_{hydra}$ as a paleoenvironmental proxy. Porewater solute concentrations indicate that these authigenic carbonate minerals form in a narrow and shallow zone where Ca and DIC are both relatively enriched. Coupling $\delta^{13}C$ of ikaite crystals and $\delta^{13}C$ of porewater DIC, allows estimation of formation depth for individual crystal. The ikaite formation depths are then used to calculate the time of crystallization relative to the ambient sediments. $\delta^{18}O_{hydra}$ and $\delta^{18}O_{CaCO3}$ throughout JPC2 at Firth of Tay are reported. The youngest crystal precipitated in modern porewater validates the fractionation factor obtained in the previous study (Rickaby et al., 2006). The late Holocene climate pattern inferred from $\delta^{18}O_{hydra}$ and $\delta^{18}O_{CaCO3}$ is comparable to other records from the region and our ikaite record provides new support that the MWP and LIA might have influenced the AP. In the future, paired $\delta^{18}O_{hydra}$ and $\delta^{18}O_{CaCO3}$ may be used to calculate $\delta^{18}O$ of paleo-porewater indicating temperature changes. At this stage, the geochemistry of ikaite serves as a qualitative, rather than a quantitative, climatic proxy, because it remains challenging to account for kinetic effects on uptake of $\delta^{18}O$ into the carbonate during crystallization and any post-crystallization exchange of $\delta^{18}O_{hydra}$ signal.

Acknowledgments

We are grateful to the scientific party and crew members of NBP0703. Bradley Michalchuk, Rice University, shared detailed core description. We thank Bastian Georg, Norman Charnley and Stathys Papadimitriou, for help on technical issues. The manuscript was improved by comments from three anonymous reviewers and the editor Gideon Henderson. This work is supported by Natural Environment Research Council (NERC award NE/E014801/1).

Appendix A. Supplementary data

Supplementary data to this article can be found online at doi:10.1016/j.epsl.2012.01.036.

References

Adkins, J.F., et al., 2002. The salinity, temperature, and delta O-18 of the glacial deep ocean. Science 298 (5599), 1769–1773.
Bentley, M.J., et al., 2009. Mechanisms of Holocene palaeoenvironmental change in the Antarctic Peninsula region. Holocene 19 (1), 51–69.
Bischoff, J.L., et al., 1993. The solubility and stabilization of ikaite (Caco3.6H2O) from 0-degrees-C to 25-degrees-C — environmental and paleoclimatic implications for thinolite tufa. J. Geol. 101 (1), 21–33.
Brachfeld, S., et al., 2003. Holocene history of the Larsen-A Ice Shelf constrained by geomagnetic paleointensity dating. Geology 31 (9), 749–752.
Buchardt, B., et al., 1997. Submarine columns of ikaite tufa. Nature 390 (6656), 129–130.
Council, T.C., Bennett, P.C., 1993. Geochemistry of ikaite formation at Mono Lake, California — implications for the origin of tufa mounds. Geology 21 (11), 971–974.
Dietzel, M., et al., 2009. Oxygen isotopic fractionation during inorganic calcite precipitation — effects of temperature, precipitation rate and pH. Chem. Geol. 268 (1–2), 107–115.

Domack, E.W., et al., 2007. Spatial and Temporal Distribution of Ikaite Crystals in Antarctic Glacial Marine Sediments. USGS Open-File Report 2007–1047. . Extended Abstract 015, 5 p.
Domack, E.W., Ishman, S., 1993. Oceanographic and physiographic controls on modern sedimentation within Antarctic fjords. Geol. Soc. Am. Bull. 105 (9), 1175–1189.
Domack, E.W., et al., 1995. Late Holocene advance of the Muller Ice Shelf, Antarctic Peninsula — sedimentological, geochemical and paleontological evidence. Antarct. Sci. 7 (2), 159–170.
Greinert, J., Derkachev, A., 2004. Glendonites and methane-derived Mg-calcites in the Sea of Okhotsk, Eastern Siberia: implications of a venting-related ikaite/glendonite formation. Mar. Geol. 204 (1–2), 129–144.
Hall, B.L., et al., 2010. Reduced ice extent on the western Antarctic Peninsula at 700–970 cal. yr BP. Geology 38 (7), 635–638.
Hansen, M.O., et al., 2011. The fate of the submarine ikaite tufa columns in southwest Greenland under changing climate conditions. J. Sediment. Res. 81, 553–561.
Hensen, C., et al., 2003. Control of sulfate pore-water profiles by sedimentary events and the significance of anaerobic oxidation of methane for the burial of sulfur in marine sediments. Geochim. Cosmochim. Acta 67 (14), 2631–2647.
Heroy, D.C., et al., 2008. Holocene climate change in the Bransfield Basin, Antarctic Peninsula: evidence from sediment and diatom analysis. Antarct. Sci. 20 (1), 69–87.
Jansen, J.H.F., et al., 1987. Ikaite pseudomorphs in the Zaire deep-sea fan — an intermediate between calcite and porous calcite. Geology 15 (3), 245–248.
Jones, V.J., et al., 2000. Palaeolimnological evidence for marked Holocene environmental changes on Signy Island, Antarctica. Holocene 10 (1), 43–60.
Khim, B.K., et al., 2002. Unstable climate oscillations during the late Holocene in the eastern Bransfield Basin, Antarctic Peninsula. Quat. Res. 58 (3), 234–245.
Kim, S.T., ONeil, J.R., 1997. Equilibrium and nonequilibrium oxygen isotope effects in synthetic carbonates. Geochim. Cosmochim. Acta 61 (16), 3461–3475.
Leventer, A., et al., 2002. Laminations from the Palmer Deep: a diatom-based interpretation. Paleoceanography 17 (2) -.
Leventer, A., et al., 1996. Productivity cycles of 200–300 years in the Antarctic Peninsula region: understanding linkages among the sun, atmosphere, oceans, sea ice, and biota. Geol. Soc. Am. Bull. 108 (12), 1626–1644.
Liu, X.D., et al., 2005. A 1300-year record of penguin populations at Ardley Island in the Antarctic, as deduced from the geochemical data in the ornithogenic lake sediments. Arct. Antarct. Alp. Res. 37 (4), 490–498.
Lu, Z.L., et al., 2010. Pore fluid modeling approach to identify recent meltwater signals on the west Antarctic Peninsula. Geochem. Geophys. Geosyst. 11 -.
Majewski, W., Anderson, J.B., 2009. Holocene foraminiferal assemblages from Firth of Tay, Antarctic Peninsula: paleoclimate implications. Mar. Micropaleontol. 73 (3–4), 135–147.
Michalchuk, B.R., et al., 2009. Holocene climate and glacial history of the northeastern Antarctic Peninsula: the marine sedimentary record from a long SHALDRIL core. Quat. Sci. Rev. 28 (27–28), 3049–3065.
Milliken, K.T., et al., 2009. High-resolution Holocene climate record from Maxwell Bay, South Shetland Islands, Antarctica. Geol. Soc. Am. Bull. 121 (11–12), 1711–1725.
Monien, P., et al., 2011. A geochemical record of late Holocene palaeoenvironmental changes at King George Island (maritime Antarctica). Antarct. Sci. 23 (3), 255–267.
Pudsey, C.J., Evans, J., 2001. First survey of Antarctic sub-ice shelf sediments reveals mid-Holocene ice shelf retreat. Geology 29 (9), 787–790.
Rickaby, R.E.M., et al., 2006. Potential of ikaite to record the evolution of oceanic delta O-18. Geology 34 (6), 497–500.
Romanek, C.S., et al., 1992. Carbon isotopic fractionation in synthetic aragonite and calcite — effects of temperature and precipitation rate. Geochim. Cosmochim. Acta 56 (1).
Schrag, D.P., Depaolo, D.J., 1993. Determination of delta-O-18 of seawater in the deep ocean during the Last Glacial Maximum. Paleoceanography 8 (1), 1–6.
Schubert, C.J., et al., 1997. C-13 isotope depletion in ikaite crystals: evidence for methane release from the Siberian shelves? Geo-Mar. Lett. 17 (2), 169–174.
Selleck, B.W., et al., 2007. A review and synthesis of glendonites (pseudomorphs after ikaite) with new data: assessing applicability as recorders of ancient coldwater conditions. J. Sediment. Res. 77, 980–991.
Shevenell, A.E., et al., 2011. Holocene Southern Ocean surface temperature variability west of the Antarctic Peninsula. Nature 470, 250–254.
Stein, C.L., Smith, A.J., 1986. Authigenic carbonate nodules in the NankaiTrough, Site 583. Init. Rep. Deep Sea Drilling Proj. 87, 659–668.
Stenni, B., et al., 2006. EPICA Dome C Stable Isotope Data to 44.8 KYrBP, IGBP PAGES/World Data Center for Paleoclimatology, Data Contribution Series # 2006–112. NOAA/NCDC Paleoclimatology Program, Boulder CO, USA. .
Suess, E., et al., 1982. Calcium-carbonate hexahydrate from organic-rich sediments of the Antarctic shelf — precursors of glendonites. Science 216 (4550), 1128–1131.
Turner, J.V., 1982. Kinetic fractionation of C-13 during calcium-carbonate precipitation. Geochim. Cosmochim. Acta 46 (7), 1183–1191.
Vaughan, D.G., Doake, C.S.M., 1996. Recent atmospheric warming and retreat of ice shelves on the Antarctic Peninsula. Nature 379 (6563), 328–331.
Wallmann, K., et al., 2006. Kinetics of organic matter degradation, microbial methane generation, and gas hydrate formation in anoxic marine sediments. Geochim. Cosmochim. Acta 70 (15), 3905–3927.
Zabel, M., Schulz, H.D., 2001. Importance of submarine landslides for non-steady state conditions in pore water systems — lower Zaire (Congo) deep-sea fan. Mar. Geol. 176 (1–4), 87–99.